Conception and Development of a Photocatalytic Reactor for H$_2$S Degradation

Eduardo Borges Lied[a]*, Camilo Freddy Mendoza Morejon[b], Ana Paula Trevisan[c], Fábio Luiz Fronza[a], Kauanna Uyara Devens[c]

[a]Federal University of Technology Parana, Department of Biological and Environmental Sciences, Medianeira, Brazil
[b]Western Parana State University, Chemical Engineering Program, Toledo, Brazil
[c]Western Parana State University, Agricultural Engineering Program, Laboratory of Biological Reactors, Cascavel, Brazil
eduardolied@utfpr.edu.br, lied.eduardo@gmail.com

For the development of a photocatalytic reactor on an industrial scale it was evaluated the degradation of hydrogen sulphide (H$_2$S) from tests with different coatings based on TiO$_2$. The surfaces formed with these coatings were structural and morphologically characterized by scanning electron microscopy with energy dispersive X-ray (SEM-EDX) and X-ray diffraction (XRD) analysis. The flow rate, inlet concentration of H$_2$S, activation and deactivation times (saturation) were evaluated as performance parameters of the degradation reaction. Conversion rates were studied for different residence times (RT), with a conversion of up to 95 % for RT = 30 s.

1. Introduction

The use of photocatalysis using Titanium Dioxide (TiO$_2$) in environmental decontamination area has received significant attention in the past few years (Scarsella et al., 2017; Ahmad et al., 2016; Boyjoo et al., 2017), and in this context gaseous pollutants treatment area has shown a greater industrial-technological development in relation to the other environmental applications of photocatalysis (Paz, 2010; Ochiai and Fujishima, 2012). Photocatalysis is an emerging technology for depollution because it is a process that has the potential to function at ambient temperatures and at low substances concentrations. Thus, photocatalysis by TiO$_2$ presents several studies regarding the use and application in environmental area, mainly in relation to treatment and remediation of pollutants. It is possible to conclude that there is a certain predominance of photocatalysis use for the treatment of liquid-phase pollutants - water and effluent treatment - as evidenced by the works of Seynure et al. (2016) and Bekbolet et al. (1996). However, the use of photocatalytic processes for gas-phase pollutants has significant and expressive numbers, which reflects the feasibility when using this technology for the treatment of these pollutants as has been studied, for example, in Mammadov et al. (2017), Zhao (2018), Sarno and Ponticorvo (2018), Guillard et al (2007), Brancher et al. (2016), Sopyan (2007) and Alonso-Tellez et al. (2012).But, the actual implementation of this technology suffers from some technical aspects, such as the costs associated with energy sources use for artificial radiation provision (Vaiano et al., 2017), lifespan of the materials used (Garcia et al., 2017) and others. Thus, literature shows that the major problem for the implementation of photocatalytic processes in emissions treatment is related to the development and optimization of reactors in an industrial scale, where an interface with engineering is necessary.

2. Experimental part

For the degradation of the hydrogen sulphide (H$_2$S) in the gas-phase it was developed a reduced scale reactor (experimental module) incorporated with 4 types of photocatalysts. The arrangement of this experimental apparatus consisted of the following parts: air compressor (1); flow regulator (2); flowmeter (3); container with H$_2$S generating solution connected to the air dragging system (4); Alphasense® electrochemical sensor, H$_2$S-

BE model (5); photocatalytic reactor (6); radiation source (UV lamp or solar radiation) (7); and photocatalyst (8). The characterization of the experimental module was basically carried out by means of chemical and physical analyses in order to determine the main properties of the following components: (1) photocatalyst (inner surface of the module); and (2) transparent surface (upper face of the module for radiation incidence). The inner surfaces formed with these coatings were structural and morphologically characterized by scanning electron microscopy with energy dispersive X-ray (SEM-EDX), X-ray diffraction (XRD), infrared attenuated total reflection spectroscopy (FTIR-ATR), UV-Vis diffuse reflectance spectroscopy and gravimetry analysis. The optical properties of the transparent surface were analysed by UV-Vis transmittance spectroscopy. The fluid dynamics aspects were evaluated in *Comsol Multiphysics* software with the objective of optimizing the final reactor design geometry to be proposed. Preliminary simulations were performed using laminar flow and turbulent flow interfaces (k-ε model). Due to the low velocity profile resulting from the two models, in the order of 10^{-1} m s^{-1}, the laminar model was chosen as the most likely to adequately predict the flow in the reactor.

3. Results and discussion

Diffractograms of Photosan®-based paint photocatalyst samples and TiO_2 powder show the formation of TiO_2-anatase phase characteristic peak at $2\theta = 25º$. Other low intensity peaks characteristic of TiO_2-anatase were identified in $2\theta = 38º$, 48º and 55º. For the acrylic paint sample, diffractograms indicate that the pigment which composes the paint is referring to the crystallographic phase TiO_2-rutile, with peak of greater intensity in $2\theta = 27°$. The peaks of lower intensity in $2\theta = 36°$, 41°, 54° and 69° also refer to Rutile.

The impregnation procedure for photocatalysts supported on fiber cement material yielded an approximate mass amount of 3.2 g of TiO_2, 3.1 g of Fotosan® and 4.7 g of acrylic paint. Regarding TiO_2 supported on fiberglass it was possible to impregnate 0.7 g. The incorporation degree ranged from 1.09 % to 13.2 % in mass: 1.1 % (TiO_2 + fiber cement); 1.09 % (Fotosan® paint + fiber cement); 1.61 % (Acrylic paint + fiber cement) and 13.2 % (TiO_2 + fiberglass). Among produced surfaces the cheaper was fiberglass impregnated with TiO_2, with a cost of US$ 0.34. On the other hand, the surface with highest manufacturing cost was pointed at the fiber cement material impregnated with the Italian photocatalytic paint Fotosan®, whose manufacturing cost was set at US$ 1.72. In general, surfaces that used fiber cement material became more expensive products: TiO_2 + fiber cement (US$ 1.48) and acrylic paint + fiber cement (US$ 1.51). Figures 1 (a), (b), (c) e (d) shows the micrographs results performed on the photocatalysts samples.
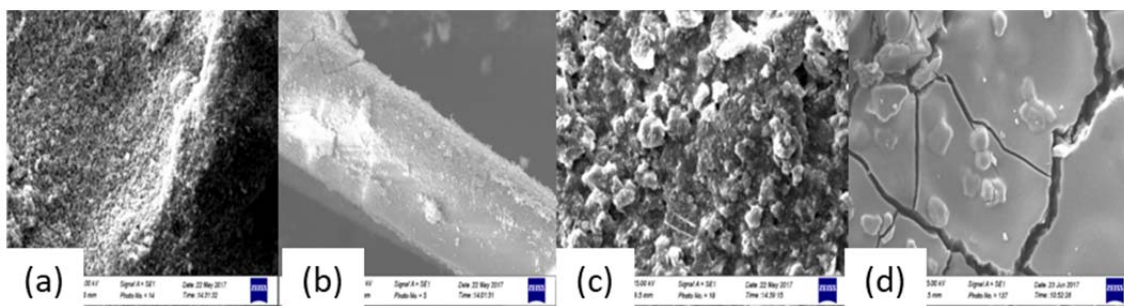

Figure 1: Micrograph of the materials surfaces: (a) fiber cement + TiO₂, (b) fiberglass + TiO₂, (c) fiber cement + acrylic paint, and (d) fiber cement + Fotosan®.

Regarding the photoactivity tests carried out by means of photocatalytic H_2S degradation tests, Table 1 shows the main results obtained.

Table 1: Overview of the photocatalytic degradation tests of H₂S using different photocatalyst materials.

Photocatalyst	Activation time (min)	Maximum efficiency (%)	Deactivation time (min)	UV radiation		Solar radiation	
				k (min^{-1})	R^2	k (min^{-1})	R^2
TiO₂ + fiberglass	12	69.0 ± 3.3	45	1.18	0.92	-	-
TiO₂ + fiber cement	7	40.9 ± 4.9	30	2.6 x 10^{-1}	0.98	-	-
Acrylic paint + fiber cement	12	90.6 ± 4.4	190	1.33	0.96	-	-
Fotosan® + fiber cement	6	77.4 ± 3.5	390	8.6 x 10^{-1}	0.99	4.4 x 10^{-1}	0.96

The acrylic paint had its photocatalytic activity significantly reduced from 190 min (3 hours and 10 min), whereas the coating based on Fotosan® presented loss of photoactivity from 390 min (6 hours and 30 min). Both have relatively high saturation times, which makes their use more prolonged, avoiding replacement or regeneration needs, important aspects for their application on an industrial scale. Besides, the material with Fotosan® paint was the only one to present photoactivity under the exposure of sunlight (Figure 2 (b)), in a way that, overall, it was concluded that Fotosan® presents the best characteristics for application on an industrial scale, in order to achieve a degradation efficiency of up to 80 % (Figure 2 (b)).

Table 1 results indicate that higher efficiencies were achieved under lower flow rate conditions, because the decrease in flow rate necessarily implies an increase in residence time. Thus, Figure 2 (a) graphically reflects the relationship between degradation efficiency and flow rate.
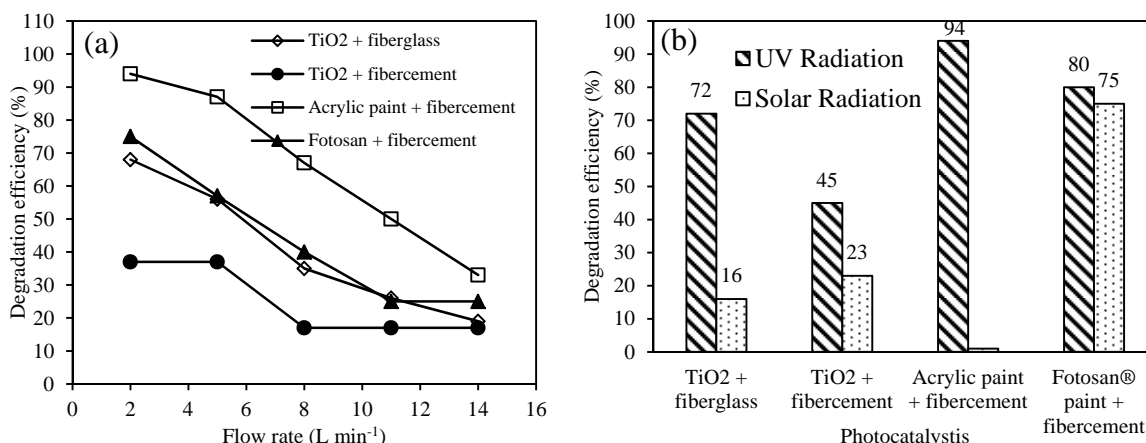

Figure 2: (a) Influence of the flow rate on photocatalytic degradation efficiency, and (b) Maximum values of degradation efficiency using UV and Solar radiation.

The transmittance measurements of transparent materials under conditions of new use are presented below (Figure 3 (a)). Figure 3 (b) shows the behaviour of transmittance properties over time ($\Delta t = 150\ d$)
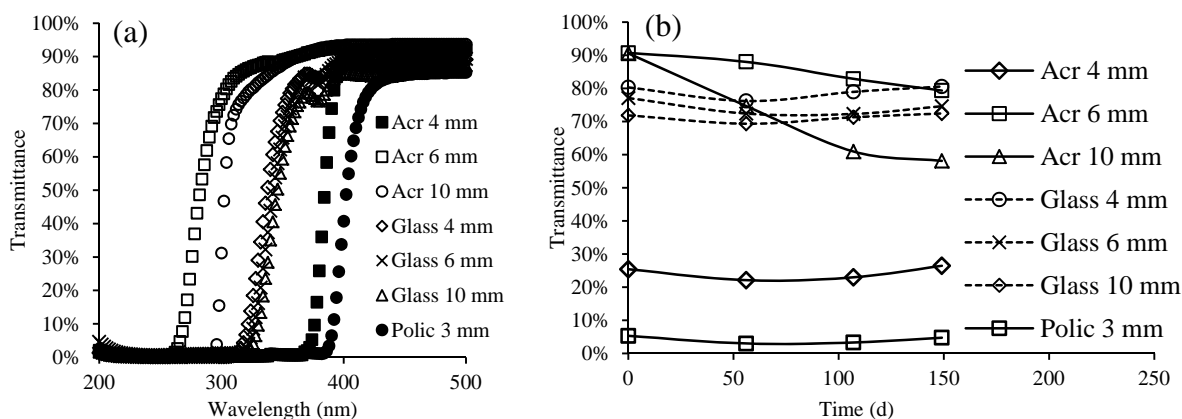

Figure 3: (a) Transmittance spectra (200 to 500 nm) of the transparent surfaces; and (b) Transmittance behaviour as a function of time within the scope of photocatalytic spectra (340 to 400 nm).

In general, the transmittance values shown in Figure 3 (b) clearly show that glass has practically not changed in its transmittance properties over time and under conditions of exposure to the weather. The acrylic material at the initial test time ("0 days") despite having transmittance properties superior to glass and polycarbonate, it is noticed that its properties suffer a significant reduction in transmittance values over time, mainly acrylic of 10 mm, which after approximately 100 days of exposure showed a significant change in transmittance.

The proposition of a reactor on an industrial scale contemplated, besides the information and parameters already obtained throughout the previous analyses, a step for definition and selection of geometry aided by

computational fluid dynamics (CFD) simulation. The best design was chosen from tests with 6 different types of arrangements (Figure 4) and 6 different types of gas supply devices, as shown in Figure 5. The selection criterion of the best arrangement was obtained based on the optimization of the residence time.
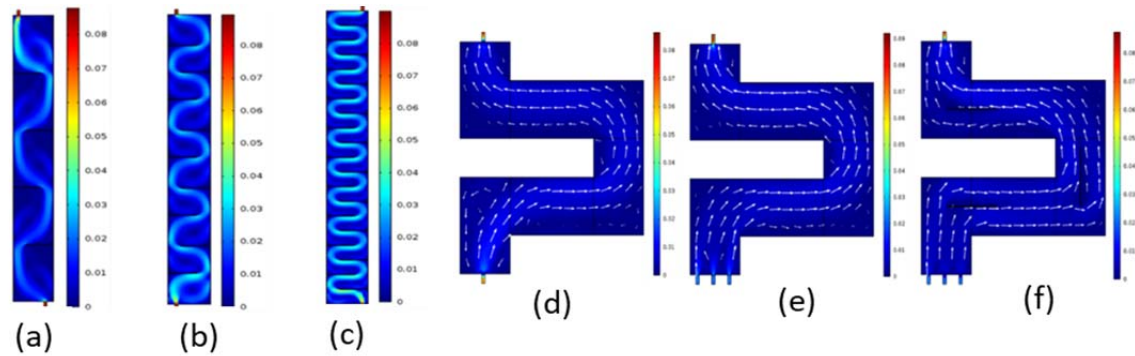

Figure 4: Speed field for rectilinear geometries with first axis tested: (a) 4, (b) 9, and (c) 19 baffles, and the rectilinear geometries with two tested axes: (d) 1, and (e) 3 input devices, (f) 3 input devices and 3 baffles.
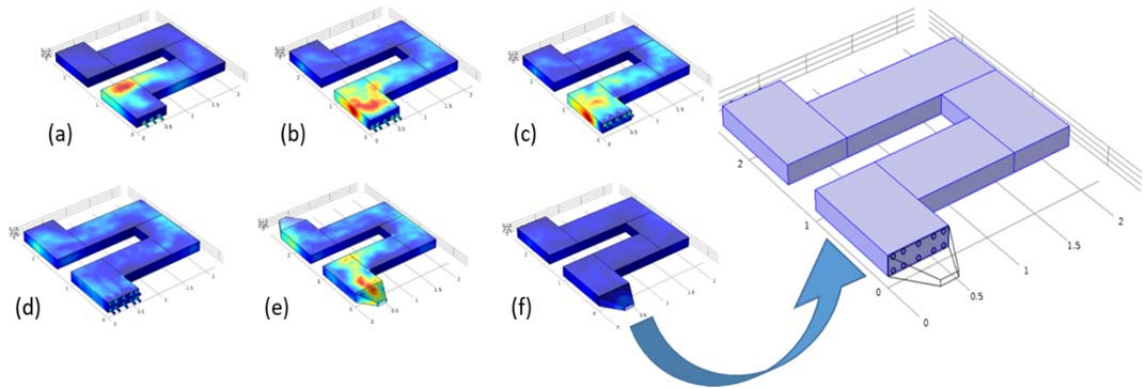

Figure 5: Speed profiles according to the arrangements of the air inletting devices: (a) lower inlet (3), (b) lower inlet (5), (c) upper inlet (5), (d) distributed inlet (10), (e) trapezoidal inlet, and (f) trapezoidal-distributed inlet (10).

Simulation results using *Comsol Multiphysics* indicated that the geometry that managed to reach a longer residence time was the geometry of Figure 4 (f), which obtained a residence time superior to the others. The increase of performance in relation to the other geometries was observed by the decrease of the average speed, an aspect attributed to the better distribution of the flow through the channel, inducing the minimization of preferential channels along the reactor.
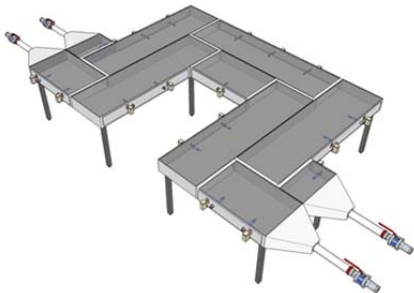
The air inletting orifices (tubes) referring to the devices shown in Figure 5 are 4 cm in internal diameter, dimensions which were useful for determining the inlet speed rate for each geometry during the simulation tests. Thus, it is fundamental to explain that Figure 5 (a) has three inlet tubes positioned in the lower portion of the reactor inlet section; Figure 5 (b) indicates 5 inlet tubes; Figure 5 (c) shows 5 tubes in the upper portion of the inlet section; Figure 5 (d) has 10 tubes (5 lower and 5 upper); Figure 5 (e) shows a different design in such a way that the air inlet has a trapezoidal style design; while Figure 5 (f) has a trapezoidal shape, but the inlet section has connected tubes.

From the results presented in Figure 5, it can be pointed out that the geometry of the air inletting device that presented the best fluid dynamic performance, from the point of view of residence time maximization, corresponded to the system with distributed inlet over 10 orifices (Figure 5 (d)), with a residence time 18 % higher than the other structures. However, this geometry with 10 inlet orifices faces a barrier from the constructive point of view, because in a real situation this device will receive the gaseous fluid from a single pipe, so it will be necessary to use another device that can make the connection between the main pipe and the inletting device. In this case, it was proposed the system shown in Figure 5 (f), which was conceived in a

hybrid system that uses the 10 inlet orifices, which is fed by the trapezoidal format device (range hood style), whose fluid dynamics simulation was performed.

Based on the results presented throughout the text it was possible to propose a system design for the elimination of H_2S through photocatalysis. Table 2 summarizes the criteria that were considered for the project and the strategies proposed from the accumulated knowledge.

Table 2: Design criteria for a photocatalytic treatment system of gas-phase pollutants.

Criteria	Proposal	Draft
Simple design: replacement of photocatalyst at the end of its lifespan life should be of easy procedure.	Multiple photocatalytic bed system that operates in semi-continuous mode, alternating in a parallel system in case of photocatalyst deactivation of the system in use.	
Economic optimization: minimal waste generation and renewable energy use.	Photocatalyst reimpregnation (transparent reactor with 4 mm thickness glass).	
Fluid contact with the photocatalyst.	High contact surface; distribution of inlet flow rate; fluid dynamic devices.	
Efficiency optimization: sufficient residence time.	Required sizing according to inlet flow rate.	
Flexibility to adapt to any fluctuations.	Modular design (parallel reactors).	
Uninterrupted operation.	Use of UV lamps.	

From the previous considerations, the proposal of photocatalytic treatment would consist of a modular system in parallel. The modular system would have an inlet device with flow rate distribution and registration valves which would allow to alternate the passage of the gaseous fluid between the main system and the backup system. UV lamps would be placed on the walls of the fluid flow channel, which would allow operation and access during maintenance periods. The photocatalyst would consist of photocatalytic paint based on TiO_2 deposited on corrugated fiber cement material.

The gaseous flow would pass through a condenser before being divided by the inlet pipes of the respective modules. Module covers shall allow the system sealing to avoid significant leaks. The height chosen for the gutter was 0.2 m (20 cm), while the width was determined to a value of 0.6 m (60 cm).

The most economical and sustainable source of radiation is solar radiation, but the limitations due to the low proportion of UV radiation in its spectral distribution, the intermittency and its variable availability encourage the use of lamps as a source of irradiation more suitable for its use in the photocatalytic treatment. The aspect of using lamp irradiation, which solves all problems arising from the use of sunlight, reduces the competitive advantage of photocatalysis as a clean and inexpensive technology. However, it was decided not to abandon the use of solar radiation during daytime periods, and to this end a versatile and innovative reactor was designed that uses both types of radiation sources simultaneously and individually. This reactor will be more efficient than a reactor with artificial radiation alone and can operate continuously without restrictions as solar radiation is available. The lamps are designed to be installed on the side walls of the module, and their maintenance would be provided through an opening system of damper door.

The module consists of two gaseous effluent flow channels: main flow gutter; and backup flow gutter. The upper part of the module is made of transparent material, so that the solar radiation can reach the photocatalyst, which is placed in the lower base of the equipment, which called the photocatalytic bed.

With a large space and easy access to its interior, the design of the reactor allows the introduction of various types of photocatalysts (photocatalytic beds) and is suitable for the use of ceramic substrates, but can receive other types of materials supports.

Inner and external walls of the reactor shall be made of materials with the following characteristics: Resistant (to withstand the pressure resulting from the gaseous fluid flow, and also resistant to weatherability); and Reflective (to increase radiation distribution along the extension and section of the reactor).

4. Conclusions

Experiments using photocatalysis (TiO$_2$/artificial and solar UV) for H$_2$S degradation have shown that this technology can be applied in the treatment of H$_2$S. Efficiencies of photocatalytic degradation of up to 95% were obtained. The results suggest that RT has a more important influence on degradation than inlet concentration.

Fotosan® paint presented high performance in both artificial and natural conditions, which makes this photocatalyst the one with higher added value among the evaluated materials.

The study of the optical properties of transparent materials concluded that the glass surface constitutes a material with significant capacity of maintenance of its optical properties, making it a product of great cost-benefit, therefore recommended for photocatalytic applications.

The fluid dynamic study indicated the best geometry in terms of longer residence time achieved, as well as the best inlet way of gaseous fluid also taking into account residence time. Among the criteria adopted for the final arrangement, the photocatalyst reimpregnation procedure was chosen as a measure that favours flexibility in the maintenance of photocatalytic systems, reducing the need for skilled labour.

Thus, photocatalysis showed to be a very promising technology in the gas-phase degradation of pollutants, so that the work developed the proposal of technical drafting of a photocatalytic equipment on an industrial scale. The design was conceived through the results obtained in the work, in such a way that the choice of materials and the final design of the equipment were performed from the reached values and parameters.

References

Ahmad R., Ahmad Z., Khan A.U., Mastoi N.R., Aslam M., Kim J., 2016, Photocatalytic systems as an advanced environmental remediation: Recent developments, limitations and new avenues for applications, Journal of Environmental Chemical Engineering, 4, 4143–4164.

Alonso-Tellez A., Robert D., Keller N., Keller V., 2012, A parametric study of the UV-A photocatalytic oxidation of H2S over TiO2, Applied Catalysis B: Environmental, 115-116, 209-218.

Boyjoo Y., Sun H., Liu J., Pareek V.K., Wang S., 2017, A review on photocatalysis for air treatment: From catalyst development to reactor design, Chemical Engineering Journal, 310, 537-559.

Brancher M., Franco D., Lisboa H.M., 2016, Photocatalytic oxidation of H2S in the gas phase over TiO2-coated glass fiber filter, Environmental Technology, 37, 2852-2864.

De La Fuente Garcia E., Carrara V., Fontana F., Natali Sora I., 2017, Simulated weathering tests of photocatalytic paint containing lafeo3, Chemical Engineering Transactions, 57, 1381-1386, DOI: 10.3303/CET1757231

Guillard C., Baldassare D., Duchamp C., Ghazzal M.N., Daniele S., 2007, Photocatalytic degradation and mineralization of a malodorous compound (dimethyldisulfide) using a continuous flow reactor, Catalysis Today, 122, 160-167.

Mammadov G., Ramazanov M., Kanaev A., Hasanova U., Huseynov K., 2017, Photocatalytic degradation of organic pollutants in air by application of titanium dioxide nanoparticles, Chemical Engineering Transactions, 60, 241-246, DOI: 10.3303/CET1760041

Ochiai T., Fujishima A., 2012, Photoelectrochemical properties of TiO2 photocatalyst and its applications for environmental purification. Journal of Photochemistry and Photobiology C: Photochemistry Reviews, 13, 247-262.

Paz Y., 2010, Application of TiO2 photocatalysis for air treatment: Patents' overview, Applied Catalysis B: Environmental, 99, 448–460.

Sarno M., Ponticorvo E., 2018, MoS2/ZnO nanoparticles for H2S removal, Chemical Engineering Transactions, 68, 481-486, DOI: 10.3303/CET1868081

Scarsella M., Bracciale M.P., De Caprariis B., De Filippis P., Petrullo A., Pronti L., Santarelli M.L., 2017, Improved photocatalytic properties of doped titanium–based nanometric oxides, Chemical Engineering Transactions, 60, 133-138, DOI: 10.3303/CET1760023

Seynure I., Aliyev F., Stoller M., Chianese A., 2016, Optimal configuration of a photocatalytic lab-reactor by using immobilized nanostructured TiO2, Chemical Engineering Transactions, 47, 199-204, DOI: 10.3303/CET1647034

Sopyan I., 2012, Kinetic analysis on photocatalytic degradation of gaseous acetaldehyde, ammonia and hydrogen sulfide on nanosized porous TiO2 films, Science and Technology of Advanced Materials, 8, 33-39.

Vaiano V., Sacco O., Sannino D., Di Capua G., Femia N., 2017, Enhanced performances of a photocatalytic reactor for wastewater treatment using controlled modulation of leds light, Chemical Engineering Transactions, 57, 553-558, DOI: 10.3303/CET1757093

Zhao L., 2018, Photocatalyst technology for deodorization in household refrigerator based on odor removal, Chemical Engineering Transactions, 68, 433-438, DOI: 10.3303/CET1868073